How to Cite: Andreev, E.V., Fadeikina, I.N., Mutali, A.K., & Kukushkin, V.I. (2025). Comparison of SERS Effect on Composite Track-Etched Membranes with Silver Nanostructures Obtained by Vacuum Deposition and Chemical Synthesis. *Eurasian Journal of Chemistry, 30, 3(119), 143-154.* https://doi.org/10.31489/2959-0663/3-25-13

Article

Received: 28 May 2025 | Revised: 14 August 2025 |
Accepted: 19 August 2025 | Published online: 21 September 2025

UCD 544.77.023.5+620.3+543.424.2

https://doi.org/10.31489/2959-0663/3-25-13

Evgeny V. Andreev[1], Irina N. Fadeikina[1, 2*], Alisher K. Mutali[1, 3], Vladimir I. Kukushkin[4]

[1]*Joint Institute for Nuclear Research, Dubna, Russia;*
[2]*Dubna State University, Dubna, Russia;*
[3]*Laboratory of Solid State Physics, The Institute of Nuclear Physics, Almaty, Kazakhstan;*
[4]*Osipyan Institute of Solid State Physics, Russian Academy of Sciences, Chernogolovka, Russia*
*(*Corresponding author's e-mail: fadeikina@yandex.ru)*

Comparison of SERS Effect on Composite Track-Etched Membranes with Silver Nanostructures Obtained by Vacuum Deposition and Chemical Synthesis

Track-etched membranes (TMs) represent a universal platform for the development of advanced sensor systems due to their tunable pore architecture, chemical functionalization, and compatibility with different nanostructures. In particular, their modification with plasmonic silver nanostructures enables the creation of efficient solid-state substrates for surface-enhanced Raman scattering (SERS), providing high sensitivity and potential for selective analyte detection. Solid substrates based on TMs can be a good compromise for SERS systems. This article is devoted to the study of the SERS effect on track-etched membranes with silver nanostructures. Silver nanostructures on track-etched membranes were obtained by thermal evaporation, magnetron sputtering think silver film with subsequent annealing. Other samples were received by deposition of colloidal silver nanoparticles stabilized with sodium citrate and β-cyclodextrin. 4-aminothiophenol was used as a test substance. All samples exhibited the SERS effect. The intensity of the Raman scattering signal in the obtained samples was compared and enhancement factors and standard deviations were estimated. Samples obtained both by deposition of nanoparticles and by sputtering show high values of the enhancement factors, which will allow them to be used in the future as substrates for biosensors.

Keywords: silver nanoparticles, track-etched membranes, vacuum deposition, surface-enhanced Raman scattering, biosensors, nanostructures, sensor system, composite

Introduction

Track-etched membranes (TMs) are a promising material for the advanced sensors development. TMs are produced from thin polymer films in which channels are created by irradiating heavy with ions and etching out destructed regions. Due to the unique technology of TMs production, they have special characteristics compared to other membranes. TMs are characterized by a uniform distribution of pore diameters, tunable pore geometry and a wide range of pore size (20 nm – 10 μm) [1]. In addition, it is possible to change the shape of pores in TMs and obtain both symmetric and asymmetric channels [2]. In addition to adjusting the structural properties, the material from which the TMs are made polyethylene terephthalate, polycarbonate, polyvinylidene fluoride, polyimide can also be selected. TMs have a wide possibility of functionalization, for example, it is possible to modify TMs with polymers [3], biomolecules [4], low molecular weight compounds [5] using functional groups on the TMs surface. It is possible to sputter metals [6], create nanofiber coatings on TMs and form metal-organic frameworks [7]. It is also possible to realize the technology of polymer grafting on TMs due to residual radicals [8]. All the above-mentioned allows to create a large number of TMs-based sensors: electrochemical sensors for heavy metal ions [9, 10], glucose [11]. In addition, nanoporous TMs are suitable for the resistive-pulse sensing method [12], to carry out digital loop mediated isothermal amplification [13]. Furthermore, sensors based on TMs with SERS-effect (surface-enhanced Raman scattering) could be designed after creating of plasmonic structures on the TMs surface [14].

Currently, SERS is a promising tool for analyzing substances, allowing the detection of extremely low concentrations down to single molecules [15]. Raman signal amplification is possible due to the formation of plasmon-polariton waves on the surface of a dielectric substrate with nanostructures plasmonic metals, or by the formation of localized plasmons ("hot spots") in colloidal solutions containing aggregates of metallic nanoparticles [16]. The most popular SERS-systems are colloidal solutions of silver nanoparticles. The main

problem of application of this type of systems is related to instability, tendency to aggregation, influence of colloidal solutions composition on Raman signal enhancement [17]. The consequence of this is the irreproducibility of measurement results and the difficulty of using colloidal systems in sensorics. Solid substrates can be a good compromise for SERS-systems.

Solid SERS-substrates are commonly based on glass, silicon or metals. The formation of nanostructures for the SERS-effect is carried out by immobilization of metal nanoparticles from solution or by deposition of metal films using PVD methods with subsequent treatment [18–22]. Recently, flexible materials such as polymer films as SERS-substrates attracted research interest due to a number of advantages. Flexible substrates are easier to manipulate and can be used with roll-to-roll technology [23, 24].

Composite silver nanoparticles and TMs show significant potential in the development of highly efficient SERS-systems. Of particular importance is the ability of TM not only to act as a flexible substrate for the preparation of SERS-active nanostructures, but also the ability to concentrate the analyte. Even without modification, TMs can be used in the design of sensors for filtration of analyte [25, 26]. Numerous works have been presented on the development of SERS-active structures on TMs. Methods for synthesis, deposition or immobilization of colloidal nanoparticles of different composition and geometry [27–30]; sputtering of metal films by PVD methods [31–33], variants of using TMs as templates for the formation of nanostructures in pores with subsequent membrane etching [34, 35]. TMs with aptamer-modified SERS-surface can significantly improve the selectivity and efficiency of analysis and create an aptasensor for the virus [36].

Despite the existing studies, there is still a challenge to design robust TM-based SERS systems with high enhancement factor, signal reproducibility and homogeneity.

The aim of the present paper is to study the features of the formation of the SERS-active silver nanostructures on the TMs surface using various methods and to compare the performance characteristics for the design of high-performance analytical systems.

Experimental

Reagents and Materials

The following reagents and materials were used in this work: sodium citrate 5.5-hydrate $Na_3C_6H_5O_7 \cdot 5.5H_2O$ (98 %, PanReac); β-cyclodextrin $C_{42}H_{70}O_{35}$ (98 %, Sigma-Aldrich); Branched polyethyleneimine (PEI) (Mn = 60.000, 50 % aqueous solution, Acros Organics); 4-Aminothiophenol (4-ATP) (97 %, Sigma Aldrich); Ethanol (99.9 %, Merc); $AgNO_3$ (99.9 %, LenReaktiv); NaOH (99.9 %, LenReaktiv); Deionized water (Milli-Q, Millipore) with a resistivity of 18 MΩ·cm at 22 °C; Track-etched membranes made of polyethylene terephthalate (thickness 19 μm, pore density $2.7 \cdot 10^8$ cm^{-2}, pore diameter 0.4 μm), obtained at the Flerov Laboratory of Nuclear Reactions of the Joint Institute for Nuclear Research.

Formation of Nanostructures from Silver Nanoparticles obtained by Chemical Synthesis

Spherical silver nanoparticles were prepared using the citrate method, based on the procedure [29]. For this, 50 ml of 10^{-3} M sodium citrate solution, heated to 95 °C, was gradually added with 12.5 ml of 10^{-3} M silver nitrate solution. Before the synthesis began, 1 M sodium hydroxide solution was added to the sodium citrate solution to achieve a pH of 9.8. The resulting mixture was kept at constant stirring and temperature for one hour.

The synthesis of silver nanoparticles using β-cyclodextrin was carried out as follows [29]. A 10^{-3} M β-cyclodextrin solution was prepared and adjusted to pH 11 using 1 M NaOH. Subsequently, 10^{-3} M silver nitrate solution was gradually added while stirring at 70 °C. The solution was incubated under these conditions for 30 minutes and then left at room temperature for one day.

The TMs were washed in ethanol and water, then immersed in a 0.1 % aqueous solution of PEI and left on a laboratory shaker for 30 minutes. After modification, the TMs were washed in water for 5 minutes. Subsequently, the silver nanoparticles solution was passed through the modified TMs using an Amicon Stirred Cells filtration cell (Millipore) [37].

Formation of Silver Nanostructures by Physical Methods

Magnetron sputtering was performed using a Q 150T S (Quorum) setup. A 10 nm silver layer was deposited at an argon residual pressure of 10^{-2} mbar and a deposition rate of 5 nm/min.

Thermal evaporation was performed using a thin film deposition system Nano 38 (Kurt J. Lesker Company, Jefferson Hills, Pennsylvania, USA). A 10 nm silver layer was deposited at a pressure of $8 \cdot 10^{-7}$ Torr and a deposition rate of 2.4 nm/min.

The formation of nanostructures was achieved through annealing in a muffle furnace (Bender) at 120 °C for 10 minutes.

The deposition of silver nanoparticles on TMs was monitored spectrophotometrically using a double-beam spectrophotometer (Evolution 600, Thermo Scientific). Spectra of colloidal solutions were recorded after filtration against deionized water. Measurements were conducted at room temperature with an optical path length of 1 cm and a slit width of 2 nm.

The zeta potential of silver nanoparticles was measured using laser Doppler microelectrophoresis (Zetasizer Nano ZSP, Malvern). A U-shaped cuvette with built-in gold electrodes was used for measurements.

Scanning electron microscopy (SEM) was performed using a microscope (SU 8020, HITACHI) with a cold field emission cathode. Cross-sectional were obtained by irradiating the TMs samples with ultraviolet light until they became brittle. To improve resolution and contrast, a 5 nm-thick layer of platinum-palladium alloy was deposited on the samples by magnetron sputtering.

The geometric parameters (diameter, shape) of nanoparticles were studied using transmission electron microscopy (TEM). TEM was performed using a microscope (Talos F200iS/TEM, Thermo Scientific). Copper grid with a thin film of amorphous carbon (SPI supplies) were used as the supporting substrate. To precipitate the nanoparticles, the grid was immersed in the solution, taken out and dried. Nanoparticle sizes were calculated from the micrographs using JMicroVision 1.3.4 software.

Raman spectroscopy was used as an additional confirmation of silver nanoparticles deposition on TMs and to evaluate the possibility of using the obtained substrates for detection of the test substance. Raman spectroscopy was performed on a spectrometer R532 (Enspectr). The excitation laser wavelength was 532 nm, the spot diameter of the focused beam was 4 μm. The test substance used was 4-ATP at a concentration of 10^{-5} M in ethanol. One drop of 2 μl was applied to the membrane for measurement and left to dry completely. The enhancement factor (K_2) was calculated from a comparative experiment in which the ratio of the Raman line intensities of 4-ATP on commercially produced Enspectr substrates (with a known enhancement factor, $K_1 = 7 \cdot 10^6$) was determined. For this purpose, measurements were performed under the same laser operating conditions (radiation power density 20 mV, exposure time 300 msec, number of scans 10) on the Enspectr substrate and TMs. The intensity values of the 1435 cm^{-1} band were averaged over 5 measurements on 5 replicate samples. K_2 calculated according to the formula:

$$K_2 = K_1 \cdot N,$$

where N is the coefficient showing how many times the values of the obtained band intensities at 1435 cm^{-1} differ from each other. The standard deviation and relative standard deviation were calculated for the measured enhancement factors using the formulas:

$$S = \sqrt{\frac{\sum(x - \bar{x})}{(n-1)}};$$

$$Sr = \frac{S}{\bar{x}},$$

where $\bar{x}$ denotes the sample mean, and n represents the sample size.

Results and Discussion

The study investigated two principal approaches to obtaining SERS-active surfaces on TMs. The first approach involves the forming of nanoparticles from thin silver films through their aggregation upon heating. The second approach comprises the deposition of chemically synthesized colloidal silver nanoparticles onto the TMs surface via filtration.

Silver Nanoparticle Formation via Sputtering

Thin silver films were produced using thermal and magnetron sputtering techniques. Thermal evaporation was selected due to its ease of implementation and widespread use. A viable alternative to thermal evaporation is magnetron sputtering, which yields films with improved adhesion, greater uniformity, thickness consistency, and reduced roughness [38]. An important advantage of magnetron sputtering is lower substrate heating and the absence of droplet phase and microparticles in the deposited material flux, unlike thermal sputtering [39]. Previous research was conducted to optimize film thickness and annealing conditions for thermally deposited films [40]. It was determined that the optimal conditions for nanoparticle formation were a film thickness of 10 nm and annealing at 120 °C. Similar studies were performed for magnetron-deposited films. The findings

revealed that the optimal conditions for nanoparticle formation were identical to those of thermally deposited films, with a film thickness of 10 nm and annealing at 120 °C. Figure 1 presents micrographs of the original and annealed silver films with a thickness of 10 nm.

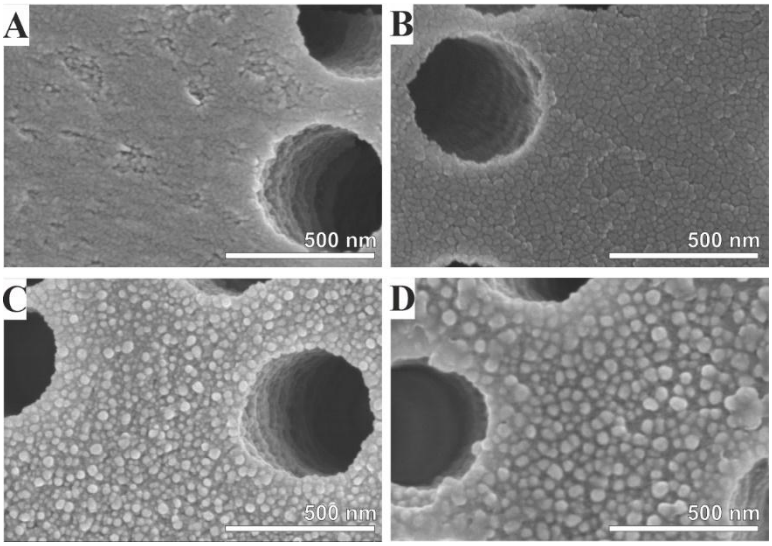

Figure 1. Micrographs obtained by SEM of a TMs with a 10 nm silver layer: Magnetron-sputtered before annealing (*A*) and after annealing (*C*); Thermal evaporation before annealing (*B*) and after annealing (*D*)

It can be observed that the initial films do not contain nanoparticles, yet a noticeable difference in morphology exists between the films produced by magnetron sputtering (Fig. 1*A*) and thermal evaporation methods (Fig. 1*B*). The films obtained via magnetron sputtering exhibit a smoother surface, while those produced by thermal evaporation show the presence of islands. These differences are inherent to the deposition methods and are typical of them.

The formation of nanostructures from thin films was achieved through heating to 120 °C, after which the film aggregated into silver nanoparticles. The nanoparticle size for films produced by magnetron sputtering (TM-Ag-M) was 21 ± 6 nm (Fig. 1*C*), whereas for films obtained by thermal evaporation (TM-Ag-T) was 28 ± 7 nm (Fig. 1*D*).

Silver Nanoparticle Deposition from Solution onto Track-Etched Membrane

The second approach to forming silver nanostructures on a TMs involved filtering a solution of nanoparticles through a PEI-modified TMs. During filtration, silver nanoparticles deposit onto the TMs surface via electrostatic and donor-acceptor interactions with PEI.

This study examined two types of silver nanoparticles. The first were nanoparticles stabilized with sodium citrate, and the second were nanoparticles stabilized with β-cyclodextrin. Both types of nanoparticles had negatively charged surfaces to prevent electrostatic repulsion from the PEI-modified TMs. The zeta potential of citrate nanoparticles was –51 ± 5 mV (pH = 10), while that of cyclodextrin nanoparticles was –35 ± 8 mV (pH = 11).

The citrate synthesis method was chosen for its simplicity, allowing for the production of nanoparticles of a specific size without the use of toxic reagents. A drawback of this method is the presence of other nanoparticle shapes, such as nanorods and triangular nanoprisms. As an alternative, the synthesis of silver nanoparticles using β-cyclodextrin as a stabilizer and reducing agent was selected. This method also avoids the use of toxic reagents and produces particles with good stability and spherical shape.

A notable feature of this method is the presence of a hydrophobic cavity in the β-cyclodextrin molecule, which can accommodate various molecules for applications in drug delivery systems and biosensing [41, 42]. Figure 2 presents micrographs of silver nanoparticles produced using sodium citrate (AgNPs-Cit) (Fig. 2*A*) and β-cyclodextrin (AgNPs-CD) (Fig. 2*B*).

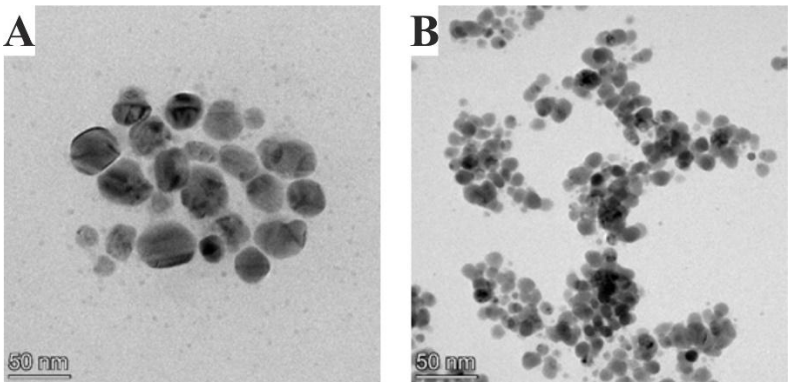

Figure 2. Micrographs of AgNPs-Cit (*A*) and AgNPs-CD (*B*) obtained by TEM

According to TEM data, the size of AgNPs-Cit and AgNPs-CD was 24 ± 10 nm and 28 ± 4 nm, respectively.

The UV-visible absorption spectra of the AgNPs-Cit and AgNPs-CD are presented in Figure 3. The characteristic plasmon resonance for silver nanoparticles was observed in the region of 400 nm.

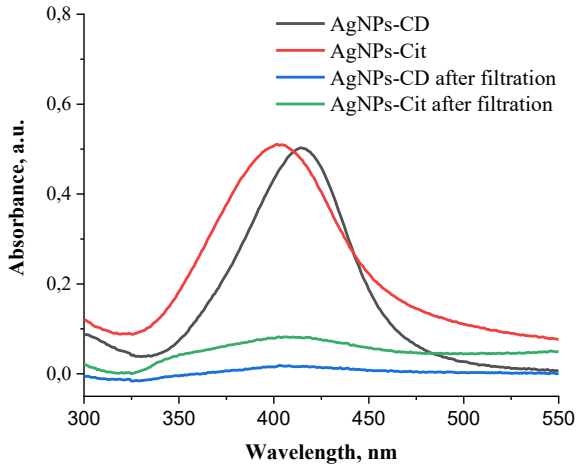

Figure 3. UV-visible absorption spectra of silver nanoparticles before and after filtration through TMs

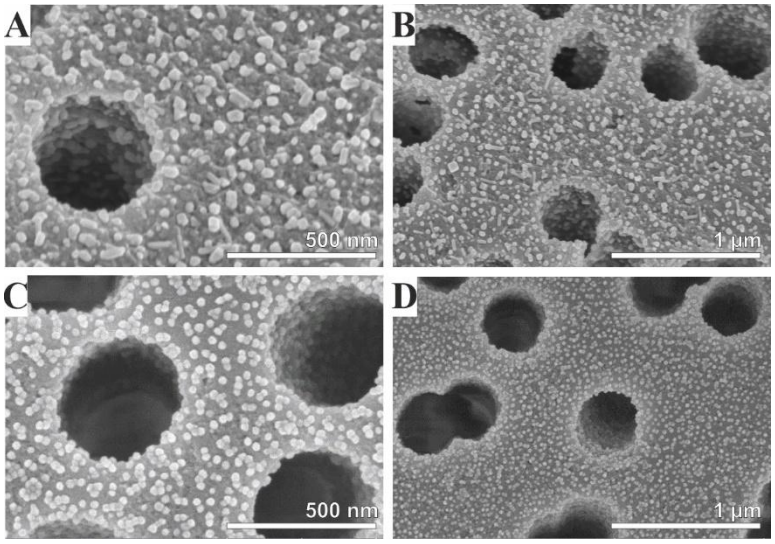

Figure 4. Micrographs of AgNPs-Cit (A, B) and AgNPs-CD (C, D) obtained by SEM

The concentration of nanoparticles was equalised by dilution based on the intensity of the plasmon resonance peak. Also, the change in intensity peak of the plasmon resonance was used to evaluate the completeness of deposition. The deposition efficiency was 90 % and 95 % for AgNPs-Cit and AgNPs-CD, respectively.

Figure 4 shows SEM of the surface of TMs after deposition AgNPs-Cit (Fig. 4 *A*, *B*) и AgNPs-CD (Fig. 4 *C*, *D*).

In the micrographs of the TMs surfaces after silver nanoparticle deposition, it can be observed that both AgNPs-Cit (Fig. 4 *A*, *B*) and AgNPs-CD (Fig. 4 *C*, *D*) are deposited uniformly across the entire surface. However, almost all nanoparticles stabilized with β-cyclodextrin are present as agglomerates on the TMs surface, while those stabilized with sodium citrate predominantly appear as single particles with lesser aggregation. In the AgNPs-Cit samples, particles of not only spherical shape but also in the form of rods, cubes, and triangular nanoprisms can be discerned.

Comparison of Chemical and Physical Approaches in the Formation of Silver Nanostructures on Track-Etched Membranes

When comparing the approaches to the formation of silver nanostructures on track-etched membranes, the depth of nanoparticle deposition in the pores, the intensity of the giant Raman scattering signal, and the relative standard deviation of the amplification coefficient were assessed. Micrographs of TMs cross-sections at angles of 90° and 70° are presented in Figure 5.

The fundamental difference in the coatings can be observed in the cross-sections of TMs with silver nanoparticles obtained via physical and chemical methods. When nanoparticles are produced from sputtered films, predominantly only the frontal surface of the TMs is filled. Within the pores, a small number of nanoparticles are observed from one edge, with deposition depths of approximately 1 μm for TM-AgNPs-T (Fig. 5*A*, *B*) and 0.5 μm for TM-AgNPs-M (Fig. 5*C*, *D*).

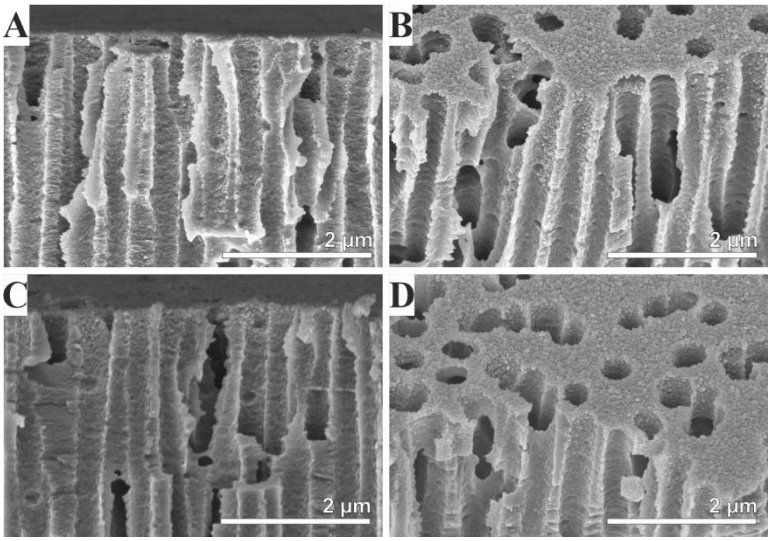

Figure 5. Micrographs of TMs cross-sectional by SEM: TM-AgNPs-T (*A*, *B*), TM-AgNPs-M (*C*, *D*)

The location of nanoparticle formation can be associated with different positions of the silver target when obtaining films relative to different sections of the membrane. The depth of nanoparticle location is also affected by different slopes of the pore channels of the TMs. With distance from the front surface, the thickness of the deposited film decreases, and as a consequence, the size and density of the particle distribution decrease. Nanoparticles are present, as a rule, at one edge of the pore, and at different depths. Part of the pore channel is inaccessible for filling with nanoparticles. The filling of membrane surface areas is schematically shown in Figure 6 (*A*).

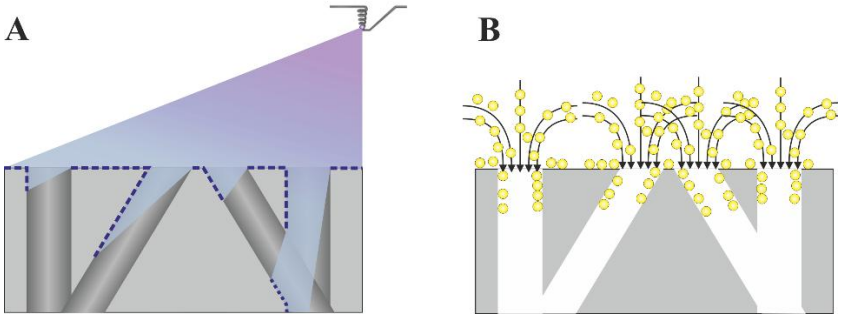

Figure 6. Schematic representation of the process of deposition of silver films (*A*) and the process of filtration of silver nanoparticles through a TMs (*B*)

Formation of a nanoparticle layer by precipitation from a solution differs fundamentally from the method of formation from thin films. The presence of silver nanoparticles both on the front surface and in the pores of the track-etched membranes, down to a depth of 3 μm, is observed on the cross-sectional of the TM-AgNPs-Cit (Fig. 7 *A*, *B*) and TM-AgNPs-CD (Fig. 7 *C*, *D*) samples.

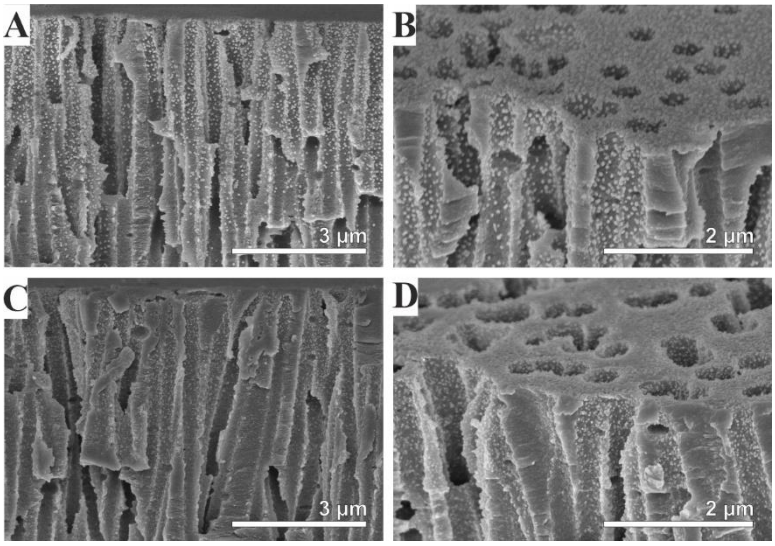

Figure 7. Micrographs of TMs cross-sectional by SEM: TM-AgNPs-Cit (*A*, *B*), TM-AgNPs-CD (*C*, *D*)

The density of the nanoparticles layer in the pore is comparable to the density of nanoparticles on the front surface of the TMs. This behavior of the nanoparticles can be associated with the fact that during filtration, the nanoparticles carried away by the flow move along the pore channel for a significant distance. At the same time, the amount of nanoparticles in the solution is sufficient to densely fill the front surface of the TMs and the pore channels (Fig. 6 *B*).

SERS Effect on Track-Etched Membranes with Silver Nanostructures

The SERS effect was studied on the composite TMs with silver nanostructures. The polymer material of the track membrane does not interfere with analyte detection due to the layer of silver nanoparticles on the surface. 4-ATP with a concentration of 10^{-5} M was used as a test substance. Due to the presence of a thiol group, 4-ATP is well adsorbed on the surface of silver nanoparticles. The presence of a benzene ring increases the SERS activity of the substance. These factors make 4-ATP a common standard for measuring the SERS signal [43].

The averaged Raman spectra of 4-ATP on samples SERS-substrates are shown in Figure 8.

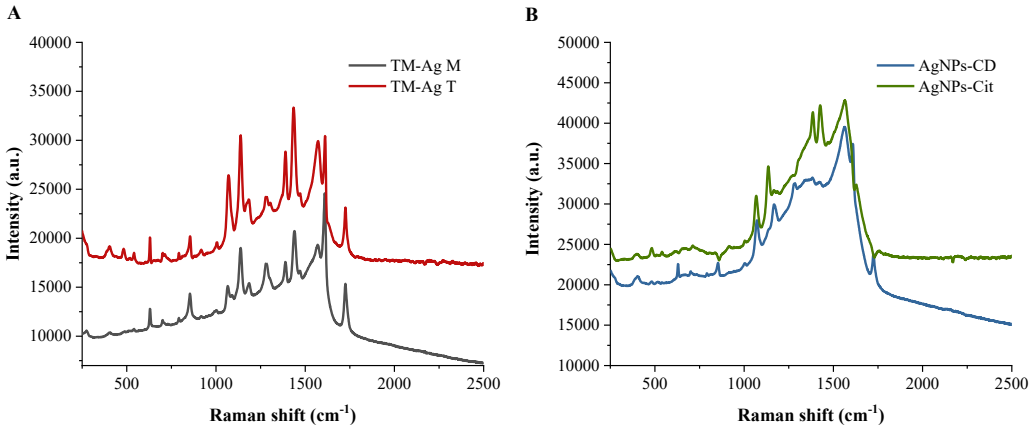

Figure 8. Raman spectra of 4-ATP (10^{-5}M): TM-Ag-T, TM-Ag-M (A); TM-AgNPs-Cit, TM- AgNPs-CD (B)

All samples of TMs exhibit vibrational bands corresponding to 4-ATP in the regions of 1145, 1390, 1435, 1575 cm^{-1}, which are consistent with similar bands from the literature data obtained on silver nanoparticles upon excitation by a laser with a wavelength of 532 nm [44]. The intensities of the Raman scattering signals were comparable. The maximum signal intensity was observed on the TM-Ag-T sample obtained by thermal evaporation, and the minimum Raman signal intensity was recorded for the TM-AgNPs-CD sample. Higher signal intensities on TMs with nanoparticles obtained from thin films can be explained by a denser arrangement of silver nanoparticles. For TM-Ag-T, the average density of nanoparticles on the front surface was ≈ 700 pcs/μm^2, for TM-AgNPs-CD ≈ 600 pcs/μm^2.

Based on the averaged Raman spectra, the enhancement factors and their relative standard deviations were calculated, the values of which are presented in Figure 9.

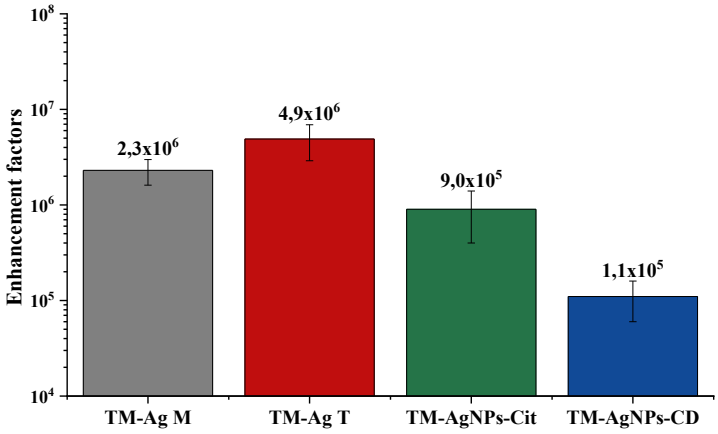

Figure 9. Histogram of the enhancement factors values
on the samples TM-Ag-T, TM-Ag-M, TM-AgNPs-Cit, TM-AgNPs-CD

The enhancement factors on TMs were determined to be $2.3 \cdot 10^6 \pm 30$ %, $4.9 \cdot 10^6 \pm 41$ %, $9.0 \cdot 10^5 \pm 56$ %, and $1.1 \cdot 10^5 \pm 45$ % for TM-Ag M, TM-Ag T, TM-AgNPs-Cit, and TM-AgNPs-CD, respectively.

It can be observed that TMs with silver nanoparticles produced by physical methods exhibited lower relative standard deviations compared to samples containing nanoparticles produced by chemical methods. The lowest relative standard deviation was achieved with magnetron sputtering samples, which can be attributed to the more homogeneous structure and uniform thickness distribution of the initial films.

The highest standard deviation was observed for TMs with silver nanoparticles synthesized using sodium citrate. This phenomenon can be explained by the greater polydispersity and presence of non-spherical shapes in citrate-stabilized silver nanoparticles.

For TM-AgNPs-Cit and TM-AgNPs-CD, there are fewer nanoparticles on the surface, but particles within the pores also contribute to the signal enhancement, which results in a higher relative standard deviation of the enhancement factor.

It can be noted that the enhancement factors of all samples are comparable in magnitude and are consistent with the enhancement values observed on other non-porous SERS substrates with silver nanostructures [45, 46].

Conclusions

Creation of a composite material based on TMs and silver NPs with the SERS effect was carried out using thermal evaporation, magnetron sputtering and deposition from solution. It was demonstrated that physical deposition methods (magnetron sputtering and thermal evaporation) enable the creation of a homogeneous coating of the frontal surface with silver nanoparticles, wherein the particles are in close contact with each other. However, within the pores, the nanoparticles formed unevenly, with the filling dependent on the position of the target relative to the examined track-etched membranes region.

Comparison of thermal evaporation and magnetron sputtering methods shows that silver nanostructures capable of exhibiting the SERS effect are formed in both cases. However, magnetron sputtering demonstrates better reproducibility of the analytical signal.

Filtration of the solution containing chemically synthesized nanoparticles through the porous material allows covering the surface with a complex relief with a sufficiently dense layer of nanoparticles and depositing the nanoparticles into the pores. The filling of the pore channels with nanoparticles occurs uniformly and to a greater depth compared to sputtering.

The highest enhancement factor of $4.9 \cdot 10^6 \pm 41$ % was achieved with the sample featuring thermal evaporation of a silver film followed by annealing. Track-etched membranes with citrate silver nanoparticles had the highest value of the relative standard deviation of the enhancement factor, $9.0 \cdot 10^5 \pm 56$ %. The obtained enhancement factors were comparable to those of other substrates.

Funding

This research was funded by the Russian Science Foundation, grant No. 24-65-00015 (https://rscf.ru/project/24-65-00015) and JINR Project No 07-5-1131-2-2024/2028.

*Author Information**

**The authors' names are presented in the following order: First Name, Middle Name and Last Name*

Evgeny Valerievich Andreev — Junior Researcher, Flerov Laboratory of Nuclear Research, Joint Institute for Nuclear Research, 141980, Dubna, Russia; e-mail: evandreev@jinr.ru; https://orcid.org/0009-0003-6924-2622

Irina Nikolaevna Fadeikina (*corresponding author*) — Candidate of Technical Sciences, Researcher, Flerov Laboratory of Nuclear Research, Joint Institute for Nuclear Research, 141980, Dubna, Russia; Dubna State University; e-mail: fadeikina@yandex.ru; https://orcid.org/0009-0006-5094-6760

Alisher Kassymbekuly Mutali — Researcher, Flerov Laboratory of Nuclear Research, Joint Institute for Nuclear Research, 141980, Dubna, Russia; Laboratory of Solid State Physics, Institute of Nuclear Physics, 050032 Almaty, Kazakhstan; e-mail: mutali@jinr.ru; https://orcid.org/0000-0003-2889-5785

Vladimir Igorevich Kukushkin — Candidate of Physical and Mathematical Sciences, Senior scientist, Osipyan Institute of Solid State Physics, Russian Academy of Sciences, Chernogolovka, Russia; e-mail: kukushvi@mail.ru; https://orcid.org/0000-0001-6731-9508

Author Contributions

The manuscript was prepared with contributions from all authors, and all authors have approved the final version for submission. CRediT: ***Evgeny Valerievich Andreev*** writing — original draft, investigation, formal analysis, review & editing, conceptualization; ***Irina Nikolaevna Fadeikina*** writing — original draft, investigation, formal analysis, review & editing, project administration, conceptualization; ***Alisher Kassymbekuly Mutali*** writing — review, investigation; ***Vladimir Igorevich Kukushkin*** writing — review, investigation.

Acknowledgments

The authors thank O. Orelovich for the help with SEM examination of track-etched membrane samples, scientific supervisor A. Nechaev for support and stimulating ideas, Prof. P. Apel for fruitful discussions and critical review of the manuscript.

Conflicts of Interest

The authors declare no conflict of interest.

References

1 Apel, P. Y. (2018). Fabrication of functional micro- and nanoporous materials from polymers modified by swift heavy ions. *Radiation Physics and Chemistry*, 159, 25–34. https://doi.org/10.1016/j.radphyschem.2019.01.009

2 Apel, P.Yu., Blonskaya, I.V., Dmitriev, S.N., Orelovich, O.L., & Sartowska, B.A. (2015). Ion track symmetric and asymmetric nanopores in polyethylene terephthalate foils for versatile applications. *Nuclear Instruments and Methods in Physics Research Section B*, 359, 1–7. https://doi.org/10.1016/j.nimb.2015.07.016

3 Fadeikina, I.N., Andreev, E.V., & Kristavchuk, O.V., et al. (2023). Electric Discharge Synthesis of Colloidal Silver Nanoparticle Solutions Using Various Modifiers for Immobilization on the Surface of Track-Etched Membranes. *Inorganic Materials*, 59(3), 337–347. https://doi.org/10.1134/s0020168523030056

4 Zarubin, M., Andreev, E., Kravchenko, E., et al. (2024). Developing tardigrade-inspired material: Track membranes functionalized with Dsup protein for cell-free DNA isolation. *Biotechnology Progress*. https://doi.org/10.1002/btpr.3478

5 Yamauchi, Y., Blonskaya, I.V., & Apel, P.Y. (2017). Adsorption of nonionic surfactant on porous and nonporous poly(ethylene terephthalate) films. *Colloid Journal*, 79(5), 707–714. https://doi.org/10.1134/S1061933X17050167

6 Rossouw, A., Vinogradov, I.I., Serpionov, G.V., Gorberg, B.L., Molokanova L.G., & Nechaev A.N. (2022). Composite Track Membrane Produced by Roll Technology of Magnetron Sputtering of Titanium Nanolayer. *Bulletin of the Russian Academy of Sciences: Physics*, 86(3), 251–255. https://doi.org/10.1134/S2517751622030039

7 Ponomareva O.Y., Drozhzhin N.A., Vinogradov I.I., Vershinina T.N., Altynov V.A., Zuba I., Nechaev A.N., & Pawlukojć, A. (2024). Metal-organic framework based on nickel, L-tryptophan and 1,2-bis(4-pyridyl)ethylene, consolidated on a track-etched membrane. *Bulletin of the Russian Academy of Sciences: Physics*, 88(6), 543–547. https://doi.org/:10.31857/S0044457X24060132

8 Pinaeva, U., Lairez, D., Oral, O., et al. (2019). Early warning sensors for monitoring mercury in water. *Journal of Hazardous Materials*, 375, 120–128. https://doi.org/10.1016/j.jhazmat.2019.05.023

9 Pinaeva, U., Dietz, T.C., & Sheikhly M. Al. (2019). Bis[2-(methacryloyloxy)ethyl]phosphate radiografted into track-etched PVDF for uranium (VI) determination by means of cathodic stripping voltammetry. *Reactive and Functional Polymers*, 140, 104–112. https://doi.org/10.1016/j.reactfunctpolym.2019.06.006

10 Zhumanazar, N., Korolkov, I.V., & Yeszhanov, A.B. (2022). Enhancement of electrochemical detection of Pb^{2+} by sensor based on track-etched membranes modified with interpolyelectrolyte complexes. *Sensors and Actuators B: Chemical*, 353, 114094. https://doi.org/10.1016/j.sna.2022.114094

11 Zhumanazar, N., Korolkov, I.V., & Yeszhanov, A.B. (2023). Electrochemical sensors based on modified track–etched membrane for non-enzymatic glucose determination. *Microchemical Journal*, 188, 109003. https://doi.org/10.1016/j.microc.2023.109003

12 Kaya, D. & Keçeci, K. (2020). Track-Etched Nanoporous Polymer Membranes as Sensors: A Review. *Journal of The Electrochemical Society*, 167(11), 070525. https://doi.org/10.1149/1945-7111/ab67a7

13 Lin, X., Huang, X., Urmann, K., Xie, X., & Hoffmann, M.R. (2019). Digital Loop-Mediated Isothermal Amplification on a Commercial Membrane. *ACS Sensors*, 4(1), 242–249. https://doi.org/10.1021/acssensors.8b01419

14 Taurozzi, J.S. & Tarabara, V.V. (2006). Support as Flow-Through Optical Sensors for Water Quality Control. *Environmental Engineering Science*, 24(1), 122–131. https://doi.org/10.1089/ees.2007.24.122

15 Gao, T., Yachi, T., Shi, X., Sato, R., Sato, C., Yonamine, Y., Kanie, K., Misawa, H., Ijiro, K., & Mitomo, H. (2024). Ultrasensitive surface-enhanced Raman scattering platform for protein detection via active delivery to nanogaps as a hotspot. *ACS Nano*, 18(32), 21593–21606. https://doi.org/10.1021/acsnano.9b04224

16 Pilot, R., Signorini, R., Durante, C., Orian, L., Bhamidipati, M., & Fabris, L. (2019). A Review on Surface-Enhanced Raman Scattering. *Biosensors*, 9(2), 57. https://doi.org/10.3390/bios9020057

17 Aroca, R. F., Alvarez-Puebla, R. A., Pieczonka, N., et al. (2005). Surface-enhanced Raman scattering on colloidal nanostructures. *Advances in Colloid and Interface Science*, 116, 45. https://doi.org/10.1016/j.cis.2005.04.007

18 Mahanty, S., Majumder, S., Paul, R., Boroujerdi, R., Valsami-Jones, E., & Laforsch, C. (2024). A review on nanomaterial-based SERS substrates for sustainable agriculture. *Science of The Total Environment*, 884, 174252. https://doi.org/10.1016/j.scitotenv.2024.174252

19 Peng, J., Song, Y., Lin, Y., & Huang, Z. (2024). Introduction and Development of Surface-Enhanced Raman Scattering (SERS) Substrates: A Review. *Nanomaterials*, 14(20), 1648. https://doi.org/10.3390/nano14201648

20 Huang, Y., Yuan, B., Wang, X., Dai, Y., Wang, D., Gong, Z., Chen, J., Shen, L., Fan, M., & Li, Z. (2023). Industrial wastewater source tracing: The initiative of SERS spectral signature aided by a one-dimensional convolutional neural network. *Water Research*, 232, 119662. https://doi.org/10.1016/j.watres.2023.119662

21 Parnsubsakul, A., Ngoensawat, U., Wutikhun, T., Sukmanee, T., Sapcharoenkun, C., Pienpinijtham, P., & Ekgasit, S. (2020). Silver nanoparticle/bacterial nanocellulose paper composites for paste-and-read SERS detection of pesticides on fruit surfaces. *Carbohydrate Polymers*, 235, 115956. https://doi.org/10.1016/j.carbpol.2020.115956

22 Zhang, L., Zhang, P., & Fang, Y. (2007). An investigation of the surface-enhanced Raman scattering effect from new substrates of several kinds of nanowire arrays. *Journal of Colloid and Interface Science*, 311(2), 502–506. https://doi.org/10.1016/j.jcis.2007.03.024

23 Ma, J., Zhao, J., Liu, X., Gu, C., Zeng, S., Birowosuto, M. D., Jiang, J., Jiang, T., & Wu, K. (2024). Ultrasensitive SERS-based detection of prostate cancer exosome using Cu2O–CuO@Ag composite nanowires. *Biosensors and Bioelectronics*, 243, 115775. https://doi.org/10.1016/j.bios.2023.115775

24 Mahanty, S., Majumder, S., Paul, R., et al. (2024). A review on nanomaterial-based SERS substrates for sustainable agriculture. *Science of The Total Environment*, 950, 174252. https://doi.org/10.1016/j.scitotenv.2024.174252

25 Zhdanov, G., Nyhrikova, E., Meshcheryakova, N. et al. (2022). A Combination of Membrane Filtration and Raman-Active DNA Ligand Greatly Enhances Sensitivity of SERS-Based Aptasensors for Influenza A Virus. *Frontiers in Chemistry*, 10, 937180. https://doi.org/10.3389/fchem.2022.937180

26 Wigginton, K.R. & Vikesland, P.J. (2010). Gold-coated polycarbonate membrane filter for pathogen concentration and SERS-based detection. *Analyst*, 135(4), 1320–1326. https://doi.org/10.1039/B919270K

27 Qi, X., Wang, X., Dong, Y., Xie, J., Gui, X., Bai, J., Duan, J., Liu, J., & Yao, H. (2022). Fast synthesis of gold nanostar SERS substrates based on ion-track etched membrane by one-step redox reaction. *Sensors and Actuators B: Chemical*, 364, 120955. https://doi.org/10.1016/j.saa.2022.120955

28 Zhang, R., Zhang, L., Xie, S., Yang, X., Liu, Y., Wang, M., & He, Y. (2025). A simple and rapid preparation of Au-Ag alloy nanourchins flexible membrane for ultrasensitive SERS detection of microplastics in water environment. *Sensors and Actuators B: Chemical*, 373, 126451. https://doi.org/10.1016/j.saa.2025.126451

29 Fadeikina, I. N., Andreev, E. V., Yurenkov, D. I., et al. (2024). Synthesis of silver nanoparticles for the production of hybrid track-etched membranes and their further use as sensory materials. *Russian Journal of Applied Chemistry*, 97(3), 244–250. https://doi.org/10.31857/S0044461824030071

30 Mashentseva, A.A., Sutekin, D.S., Rakisheva, S.R., & Barsbay, M. (2025). Composite Track-Etched Membranes: *Synthesis and Multifaced Applications*. https://doi.org/10.3390/polym16182616

31 Kovalets, N.P., Kozhina, E.P., Razumovskaya, I.V., Bedin, S.A., Piryazev, A.A., Grigoriev, Yu.V., & Naumov, A.V. (2022). Toward single-molecule surface-enhanced Raman scattering with novel type of metasurfaces synthesized by crack-stretching of metallized track-etched membranes. *The Journal of Chemical Physics*, 156(3). https://doi.org/10.1063/5.0078451

32 Lyu, S., Zhang, Y., Du, G., Di, C., Yao, H., Fan, Y., Duan, J., & Lei, D. (2023). Double-sided plasmonic metasurface for simultaneous biomolecular separation and SERS detection. Spectrochimica Acta Part A: *Molecular and Biomolecular Spectroscopy*, 285, 121801. https://doi.org/10.1016/j.saa.2022.121801

33 Rodrigues, D.C., Andrade, G.F.S., & Temperini, M.L.A. (2013). SERS performance of gold nanotubes obtained by sputtering onto polycarbonate track-etched membranes. *Physical Chemistry Chemical Physics*, 15(4), 1169–1176. https://doi.org/10.1039/C2CP42994A

34 Ritchie, G., Burstein, E., & Stephens, R.B. (1985). Optical phenomena at a silver surface with submicroscopic bumps. *Journal of the Optical Society of America B*, 2(4), 544–551.

35 Kozhina, E.P., Bedin, S.A., Nechaeva, N.L., Podoynitsyn, S.N., Tarakanov, V.P., Andreev, S.N., Grigoriev, Y.V., & Naumov, A.V. (2021). Ag-Nanowire bundles with gap hot spots synthesized in track-etched membranes as effective SERS substrates. *Applied Sciences*, 11(4), 1375. https://doi.org/10.3390/app11041375

36 Kukushkin, V., Kristavchuk, O., Andreev, E., et al. (2023). Aptamer-coated track-etched membranes with a nanostructured silver layer for single virus detection in biological fluids. *Frontiers in Bioengineering and Biotechnology*, 10, 1076749. https://doi.org/10.3389/fbioe.2022.1076749

37 Fadeikina, I. N., Andreev, E. V., Kristavchuk, O. V., et al. (2023). Electric discharge synthesis of colloidal silver nanoparticle solutions using various modifiers for immobilization on the surface of track-etched membranes. *Inorganic Materials*, 59(3), 337–347. https://doi.org/10.1134/s0020168523030056

38 Gudmundsson, J.T. (2020). Physics and technology of magnetron sputtering discharges. *Plasma Sources Science and Technology*, 29(11), 113001. https://doi.org/10.1088/1361-6595/abb7bd

39 Glushko, S.P. (2020). Selection of technologies for metal film application using physical deposition techniques. *Advanced Engineering Research*, 20(3), 280–288. https://doi.org/10.23947/2687-1653-2020-20-3-280-288

40 Serebrennikova, S.I., Kukushkin, V.I., Morozova, E.N., Astrakhantseva, A.S., Kristavchuk, O.V., & Nechaev, A.N. (2022). Formation of island SERS films on surfaces of track membranes and silicon substrates. *Bulletin of the Russian Academy of Sciences: Physics*, 86(4), 423–433. https://doi.org/10.3103/S1062873822040207

41 Fazylov, S.D., Nurkenov, O.A., & Nurmaganbetov, Z.S., et al. (2025). Synthesis of β-cyclodextrin-functionalized silver nanoparticles and their application for loading cytisine and its phosphorus derivative. *Molecules*, 30(6), 1337. https://doi.org/10.3390/molecules30061337

42 Yang, L., Chen, Y., Li, H., Luo, L., Zhao, Y., Zhanga, H., & Tian, Y. (2015). Application of silver nanoparticles decorated with β-cyclodextrin in determination of 6-mercaptopurine by surface-enhanced Raman spectroscopy. *Anal. Methods*, 7, 6520–6527. https://doi.org/10.1039/C5AY01212K

43 Zhu, J., Wu, N., Zhang, F., et al. (2018). SERS detection of 4-Aminobenzenethiol based on triangular Au-AuAg hierarchical-multishell nanostructure. *Spectrochimica Acta Part A: Molecular and Biomolecular Spectroscopy*, 204, 754–762. https://doi.org/10.1016/j.saa.2018.06.105

44 Ratkajec, A. & Kenđel, A. (2024). Structural characterization of 4-aminothiophenol in silver and gold colloids using surface-enhanced Raman scattering. *Croatica Chemica Acta*, 97(20), 77–85. https://doi.org/10.5562/cca4107

45 Sakir, M., Pekdemir S., Karatay A. et al (2017). Fabrication of plasmonically active substrates using engineered silver nanostructures for SERS applications. *ACS Appl. Mater. Interfaces*, 9(45), 39795–39803. https://doi.org/10.1021/acsami.7b12279

46 He, L., Riassetto, D., Bouvier, P., Rapenne, L., Chaix-Pluchery, O., Stambouli, V., & Langlet, M. (2014). Controlled growth of silver nanoparticles through a chemically assisted photocatalytic reduction process for SERS substrate applications. *Journal of Photochemistry and Photobiology A: Chemistry*, 277, 1–11. https://doi.org/10.1016/j.jphotochem.2013.12.003